

GEOHERMAL DISTRIBUTION ANALYSIS OF GEUREUDONG VOLCANO BASED ON SATELLITE DATA AND FAULT FRACTURE DENSITY (FFD)

Muhammad Isa^{*,**}, Zulfadhli^{**}, Cut Fat Thahul^{**}, Dwiky Pobri Cesarian^{**}

^{*}Department of Physics, Faculty of Science, Universitas Syiah Kuala, Banda Aceh, Indonesia, muhammadisa@unsyiah.ac.id

^{**}Department of Geophysics, Faculty of Engineering, Universitas Syiah Kuala, Banda Aceh, Indonesia zulfadhli@unsyiah.ac.id, cutfathahul@gmail.com, dwikycesarian@gmail.com

Email Correspondence : muhammadisa@unsyiah.ac.id

Received : May 31, 2021

Accepted : December 24, 2021

Published : January 16, 2022

Abstract: Geureudong Volcano area, Bener Meriah, has the potential to be developed as a renewable energy source. Analysis of the distribution of geothermal manifestations can be done with remote sensing techniques and direct measurement. Furthermore, information on geomorphological conditions, surface temperature, and geothermal potential distribution can be known based on the density value on the FFD (Fault Fracture Density) map and satellite image processing results. Data processing uses ArcGIS and ENVI software concerning geothermal manifestations. The analysis was performed by converting DEMNAS data to a hillshade for drawing straightness structures related to the fault. Image data processing to obtain vegetation density (NDVI), hydrological state (NDWI), and surface temperature distribution (LST). NDWI values are inversely proportional to NDVI. The LST value depends on the density of the vegetation; the higher the vegetation density, the lower the surface temperature. The FFD map is divided into three levels i.e. low (0-0.17 km/km²), moderate (0.17-0.47 km/km²) and high (0.47-1.2 km/km²). The distribution of geothermal potential is at medium and high-density levels, including the Silih Nara, Wih Pesam, and Pintu Rime Gayo areas. The straightness direction is in the north-south and southeast-northwest positions. Based on the NDVI, NDWI, and LST map analysis results, geothermal energy distribution has a rare to moderate vegetation density with surface temperatures ranging from 25.8°C-39.6°C. The result clearly shows that the Geureudong geothermal distribution is initial information before in situ exploration is carried out.

Keywords: NDVI; NDWI; LST; FFD

Abstrak: Gunung berapi Geureudong, Bener Meriah, sangat prospektif untuk dikembangkan terutama sebagai sumber energi terbarukan. Analisis sebaran manifestasi panas bumi dapat dilakukan dengan teknik penginderaan jauh dan pengukuran langsung. Informasi geomorfologi, temperatur permukaan dan sebaran potensi panas bumi dapat diketahui berdasarkan nilai densitas pada peta FFD (*Fault and Fracture Density*) dan hasil pengolahan citra satelit Landsat 8. Pemrosesan data menggunakan perangkat lunak ArcGIS dan ENVI yang terkait dengan manifestasi panas bumi. Analisis dilakukan dengan mengubah data DEMNAS menjadi *hillshade* untuk menggambar struktur kelurusan yang berhubungan dengan sesar. Pengolahan data citra untuk mendapatkan kerapatan vegetasi (NDVI), keadaan hidrologi (NDWI) dan distribusi suhu permukaan (LST). Nilai NDWI berbanding terbalik dengan NDVI. Nilai LST tergantung pada kerapatan vegetasi, semakin tinggi kerapatan vegetasi maka

semakin rendah suhu permukaan. Peta FFD dibagi menjadi tiga tingkatan; rendah ($0-0,17 \text{ km/km}^2$), sedang ($0,17-0,47 \text{ km/km}^2$) dan tinggi ($0,47-1,2 \text{ km/km}^2$). Sebaran potensi panas bumi berada pada tingkat kepadatan sedang dan tinggi, meliputi kawasan Silih Nara, Wih Pesam dan Pintu Rime Gayo. Arah kelurusan berada pada posisi utara-selatan dan tenggara-barat laut. Berdasarkan hasil analisis peta NDVI, NDWI dan LST didapatkan bahwa sebaran energi panas bumi memiliki kerapatan vegetasi jarang hingga sedang dengan temperatur permukaan berkisar antara 25.8°C - 39.6°C . Hasil yang diperoleh menunjukkan bahwa sebaran panas bumi Geureudong dengan sangat jelas tergambar sebagai informasi awal sebelum dilakukan eksplorasi lapangan (*in situ*).

Kata kunci: NDVI; NDWI; LST; FFD

Recommended APA Citation :

Isa, M., Zulfadhli, Thahul, C. F. & Cesarian. D., P. (2021). Geothermal Distribution Analysis of Geureudong Volcano Based On Satellite Data and Fault Fracture Density (FFD). *Elkawnie*, 7(2), 354-367.
<https://doi.org/10.22373/ekw.v7i2.9728>

Introduction

Indonesia is located at the intersection of three tectonic plates, which contributes to the availability of geothermal energy. Studying characteristics of potential geothermal areas is the first step in geothermal exploration (Sukendar et al. 1 2016). The areas in Sumatra have untapped geothermal potential, one of which is the potential found in Geureudong Volcano. This mountain is one of the active volcanoes in the Bener Meriah Regency. To explain the geothermal existence in this area, it is necessary to do an optimal analysis. Several methods for analyzing geothermal *in situ* have been widely used, such as the Gravity and Magnetic methods. However, this method is considered very limited for its wide coverage area. To improve these limitations, it is deemed necessary to analyze the distribution of geothermal energy in the Geureudong Volcano area using satellites. Remote sensing technology can provide information on geothermal potential without direct field surveys. This remote sensing technology can be done by utilizing satellites that provide data to be processed with certain software to get results that are then analyzed and used in various other applications.

The remote sensing method is an initial stage of geothermal exploration before further geoscience studies are carried out. In Indonesia, DEM data is used in the form of DEMNAS data to determine the geomorphological conditions. Based on this DEM data, an overview of the fault zone or fracture will be obtained, which is the fluid movement path. The image of this zone was known by drawing the alignment produced by the FFD (Fault Fracture Density) technique. To determine the distribution of surface temperature in the form of Land Surface Temperature (LST), Landsat 8 image data was used. Data processing begins with determining vegetation density using the Normalized Difference Vegetation Index (NDVI) technique and hydrological determination using the Normalized Difference Water Index (NDWI) technique. A vegetation density map will be obtained through this technique, a map of the hydrological state, and surface

temperature distribution to determine the zone of manifestation (Nugroho et al. 2016). This study aims to identify the geomorphological condition of the Geureudong Volcano geothermal area based on DEMNAS data. It also to see the correlation between the geothermal manifestation in the area with the level of vegetation density (NDVI), hydrological condition (NDWI), and surface temperature distribution (LST).

This research is expected to provide information on the usefulness of Landsat 8 imagery data in the initial study for potential geothermal areas. Then provide information about the relationship between straightness patterns, vegetation distribution, and surface temperature distribution with the surface geothermal manifestations scattered in Geureudong Volcano. The results of the analysis of straightness maps, vegetation distribution, and surface temperature distribution using DEM data and Landsat imagery can be used as additional references for further research and evaluation of potential geothermal reservoirs in more detail in the geothermal area found in Geureudong Volcano.

Literature Review

Geothermal energy is a clean energy source that can be an alternative energy source to replace the fossil energy. This heat energy is transferred to the earth's surface either by conduction through rocks or convection due to contact between water and heat sources (Domra *et al.*, 2015). A geothermal system is formed by four main elements: a heat source, a reservoir, a fluid that transfers heat, and a recharge area. The heat source is generally a shallow magmatic body. Usually, the magma has frozen but sometimes is still in the form of a melt. The hot fluid can appear on its own above the surface as hot springs or geysers, but most of it remains below the surface, trapped in crevices and pores of rock. Geothermal potential in an area can be seen through the potentials that appear on the surface. These potentials include hot springs, hot mud, geysers, fumaroles, solfatara, warm ground, altered rock, stress vegetation, sintered silica, and other potentials. It can be concluded that the Landsat 7 ETM+ and Landsat 8 TIRS/OLI imageries are potentially used to study the thermal status (Nasrullah, Z et al. 2020). Geothermal manifestations on the surface were thought to occur due to heat propagation from below the surface or because of the fractures that allow geothermal fluids (steam and hot water) to flow to the surface. Various geothermal manifestations are warm ground, steaming ground surface (streaming ground), hot or warm springs, hot pools, hot lakes, fumaroles, geysers, mud pools, sintered silica, and rocks that have undergone alteration. The following is an understanding of each of the surface geothermal manifestations.

Remote sensing is the science of obtaining information about objects, areas, and symptoms by analyzing data obtained from a tool without directly touching them to be studied. The satellite data were applied to extract the land surface temperature and land classification (Isa M et al. 2020).

The basic principle of the remote sensing method is any object that reflects or emits certain electromagnetic waves, depending on the physical properties or composition of the object. The four basic components of a remote sensing system are the target, the energy source, the transmission line, and the sensor. The components in this system work together to measure and record information about the target without touching the object.

The latest Landsat satellite, Landsat 8, was launched on February 11, 2013, which NASA and USGS manage. The Landsat 8 satellite is designed to carry an OLI (Operational Land Imager) imaging sensor which has one (1) near-infrared channel and seven (7) reflective, visible channels, which includes the wavelengths reflected by objects on the earth's surface, with the same spatial resolution as its predecessor Landsat, which is 30 m. To get the Land Surface Temperature in the study area, Landsat 8 imagery must go through several important stages in image processing, namely radiometric correction, brightness temperature calculation, composite band, NDVI calculation, NDWI, and LST calculations. Radiometric correction and geometric correction are necessary for processing Landsat 8 data.

Radiometric corrections are performed on OLI data to convert the sensor's Digital Number (D.N.) into spectral light. The radiometric correction was performed following Landsat 8.

$$L\lambda = ML * QCAL + AL \dots\dots\dots(1)$$

$L\lambda$ is spectral of light ($W/m^2 sr\mu m$), ML is the Radiance multiplicative scaling factor for the band, A.L. is the Radiance additive scaling factor for the band, and QCAL is the pixel value in D.N. Where, geometric corrections are made to position the image against the coordinates of objects on the earth's surface, due to the effects of the earth's rotation, the direction of the satellite's movement and the curvature of the earth's surface. The Normalized Difference Vegetation Index (NDVI) correlates between physical parameters and certain physical properties of vegetation cover (Cesarian et al., 2018). The vegetation index value was calculated from the spectral reflectance of the red band (Band 4) and NIR (Band 5) from the Landsat 8 OLI image data. The NDVI value was obtained through the following equation:

$$NDVI = RNIR - RRed / RNIR + RRed \dots\dots\dots(2)$$

The calculation of the vegetation index (NDVI) using Landsat 8 imagery was obtained through the ratio of the reflectance values of band 4 (red) and band 5 (NIR). The vegetation index was valued from -1 to 1, where according to Zhang & Li(2006), the NDVI value > 0.46 was indicated as an area covered by high-density vegetation, the value $-0.063 < NDVI < -0.185$ as water. NDVI value at a point can be obtained by extracting the histogram. The determination of the emissivity value was carried out through the NDVI (Normalized Differential Vegetation Index) method approach, where the relationship between the NDVI value and the Land Surface Emissivity (LSE) can be seen in the following table 1.

Table 1. Correlation between land cover value and ground surface emissivity value (Isaya, M., et. al. 2016)

NDVI	LSE
NDVI < -0.18	0.995
-0.18 ≤ NDVI < 0.157	0.985
0.157 ≤ NDVI ≤ 0.727	1.009 + 0.047 × ln (NDVI)
NDVI > 0.727	0.990

The Normalized Difference Water Index (NDWI) is a hydrological index that shows an area's wetness level. NDWI is a new technique developed to support NDVI. The NDWI technique aims to describe the conditions of open water features with good resolution. In its application, NDWI uses reflected infrared radiation to enhance water features and eliminate the presence of vegetation. Based on this, it is known that this technique is the opposite of the NDVI technique. If the NDVI technique (Normalized Difference Vegetation Index) displayed is the vegetation index and land cover with dark water areas, then in the NDWI technique shown are water areas with bright colors and vegetation areas with dark colors (Sisay, 2016). In processing, the NDWI technique utilizes the reflectance value in the green channel and the reflectance value in the near-infrared (NIR) channel to determine the water content contained in water bodies. This is calculated using the following equation:

$$NDWI = \frac{(GREEN - NIR)}{(GREEN + NIR)} \dots\dots\dots (3)$$

Green is the reflectance of the green channel (band 3), and Short-Wave Infrared (SWIR) reflects the short infrared channel (band 6). LST was calculated using the following equation:

$$LST = \frac{BT}{(1 + (\lambda + \frac{BT}{P}) \ln e)} \dots\dots\dots (4)$$

Where the P-value is 14380, which is obtained from the calculation of the plank constant multiplied by the value of the speed of light and divided by the Boltzmann constant so that the value of lambda is 10.8 (Maryanto et al. 1. 2016). The advantage of studying the description of subsurface temperatures can build an algorithm to develop other methods such as LST (Ugur A and Gordana J, 2016).

Digital Elevation Model (DEM) is a type of Digital Terrain Model, recording topographical or geomorphometric images of the earth's surface or other surfaces in digital format. Data DEM records elevation in raster format, then an area is divided into rectangular pixels, and elevation data is stored for each pixel in digital numbers. To obtain elevation data in geothermal areas, DEM data can be used especially for analyzing the presence of a location. In this study, the DEM data used is a grid type, so the DEM data is a sample of high surfaces in the form of a raster. (Mahmud M. and Abdullah H, 2021) Suggested that the factors that

play an essential role in determining the quality of DEM are the roughness or morphology of the terrain under study, sample or sample density, grid resolution, interpolation algorithm, vertical resolution, and terrain algorithm analysis. More DEM data were used from Shuttle Radar Topography Mission (SRTM) products than other products. The main advantage that DEM SRTM has is that it is easy to obtain. After all, it is available free of charge throughout Indonesia. SRTM DEM data is available with a spatial resolution of 90 m and 30 m, with various formats (* .HGT, * .ASCII and * .tiff). SRTM is international research pioneered by the U.S. National Geospatial-Intelligence Agency (NGA) and the U.S. National Aeronautics and Space Administration. The results of the SRTM DEM extraction can be in the form of contours, slopes, hillshades, and others. SRTM DEM data can be used for flood modeling, land conversion, greening planning, earthquake research, and ice movement in the environmental field. The SRTM DEM data can also be applied to a preliminary study for geothermal prospect areas in the energy sector. SRTM DEM extraction can find the location of faults and fractures, both of which are factors in the occurrence of geothermal sources and their hydrology.

Study Area

This research was conducted in Bener Meriah Regency, Aceh Province. Geureudong Volcano is a stratovolcano-type volcano that has an altitude of 2,624 asl. The location of Bur Ni Geureudong Volcano is at coordinates 4.81° North Latitude and 96.82° East Longitude (Barber, Crow, & Milsom, 2005). The specific study area can be seen in figure 1.

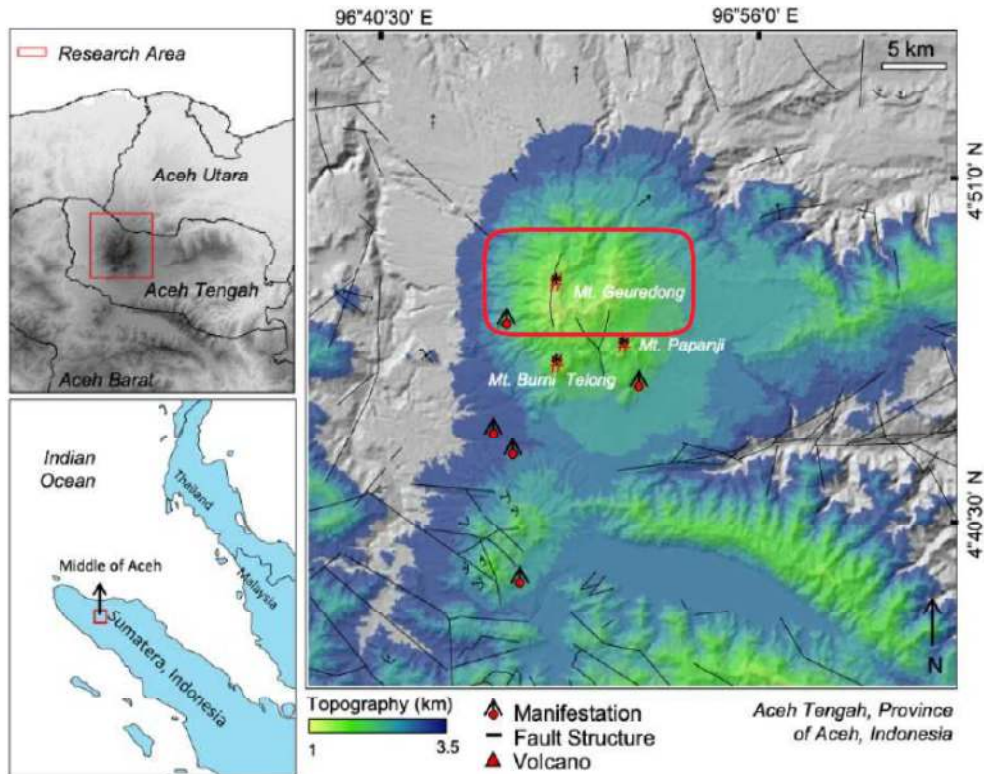


Figure 1. The map of the studi area, Mount Geureudong, Bener Meriah and Aceh Tengah

Geureudong Volcano is a large mountain complex with two young parasitic cones on the southern slopes, namely Mount Bur Ni Telong and Mount Papanji. The types of rock deposits found in the Bur Ni Geureudong area are the Enang-Enang (Qvee) volcanic rock (Cesarian et al., 2018). Bener Meriah Regency has geothermal potential, marked by fumaroles that smoke thin and weak. It three hot springs, namely Pondok Gresek Hot Springs in Bukit District, Uning Bertih Hot Springs in Lampahan Village, Wih Pesam and Hot springs in Pintu Rime Gayo District.

Methodology

The data used in this study were collected in advances, such as digital data for DEM SRTM and Landsat imagery and other important data to support this research. Digital data for DEM SRTM and Landsat imagery were downloaded at the following link <https://earthexplorer.usgs.gov/>. All data that has been collected will be processed according to its use. The first one is DEM SRTM from 3 January 2009, which has a 30-meter resolution (1-arc second). The second one is Landsat image, acquired on 18 July 2017. The projection of the imagery is UTM WGS84 with a spatial resolution of 30 m for bands 1 to 7 and 9, 15 m for band 8 (panchromatic), and 100 m for bands 10 and 11 (thermal). The two data had

different processing methods and were processed accordingly with high potential in the geothermal resource.

Landsat 8 data processing which aims to determine the value of vegetation density, the hydrological state, and the surface temperature distribution, had the first step by making corrections to the bands used for determining each of these parameters. The correction was divided into two parts. The first part was a radiometric correction for determining the hydrological state and the vegetation density. It includes converting the digital number value into a reflectant TOA value and calibrating the sun's elevation angle.

The second part was also radiometric correction for determining surface temperature distribution. The digital number value was converted into radian TOA value, and an atmosphere correction was performed in this correction. The results obtained from this process are the value of the hydrological state and the value of vegetation density depicted through the NDWI map and the NDVI map. Sequentially, the data processing stages are shown in figure 2.

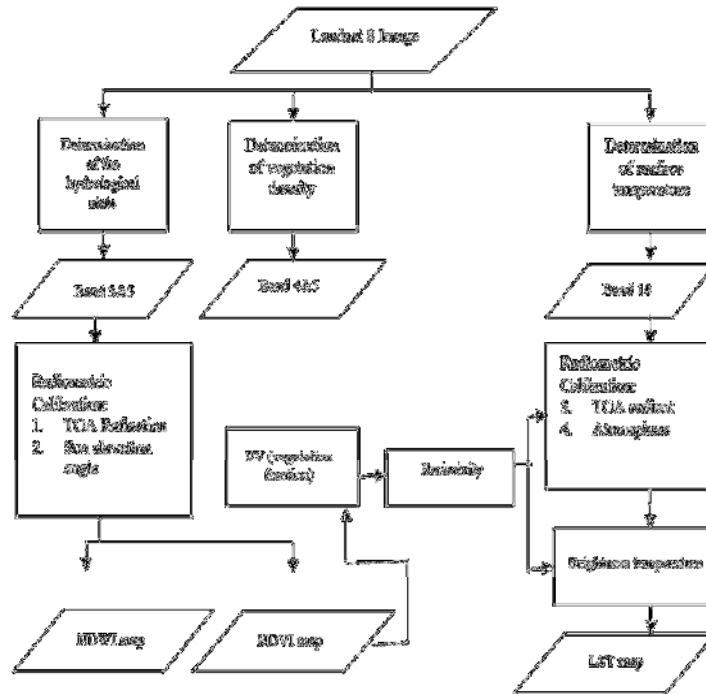


Figure 2. Landsat 8 processing flowchart

As for the surface temperature distribution value, this calculation includes determining the vegetation fraction obtained from the extraction of the vegetation density value and has been corrected with the emissivity value. This calculation will be obtained the value of the surface temperature distribution. After processing the data according to figure 2 and figure 3, the final results will be obtained in the form of an FFD map, NDWI map, NDVI map, and LST map, where the final

results will be analyzed and interpreted. The results of image processing of Landsat 8 obtained the distribution of potential geothermal areas (Naufal, F. et al. 1 2017).

This interpretation is carried out to determine the correlation or relationship between the straightness value (FFD), the value of the hydrological state (NDWI), the value of vegetation density (NDVI), and the value of the surface temperature distribution (LST) to the distribution of geothermal manifestations in the Geureudong Volcano area.

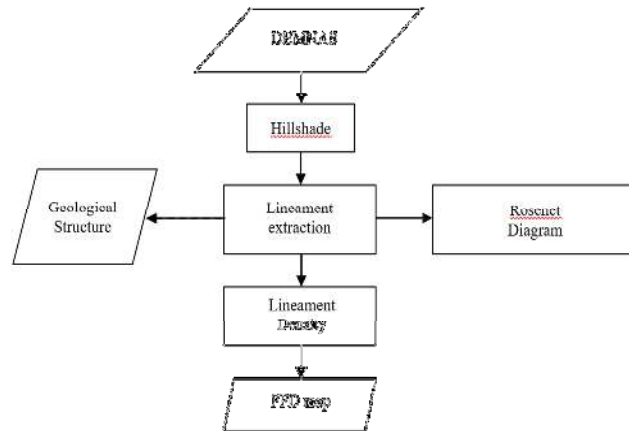


Figure 3. DEM SRTM processing flowchart

Results and Discussion

Digital Elevation Model (DEM) data in the form of DEMNAS data with a resolution of 0.27 arc-second (~8 m) used to generate FFD (Fault and Fracture Density) map in figure 4. DEMNAS with good spatial resolution can determine geomorphological and geological conditions, connection with Geureudong geothermal potential.

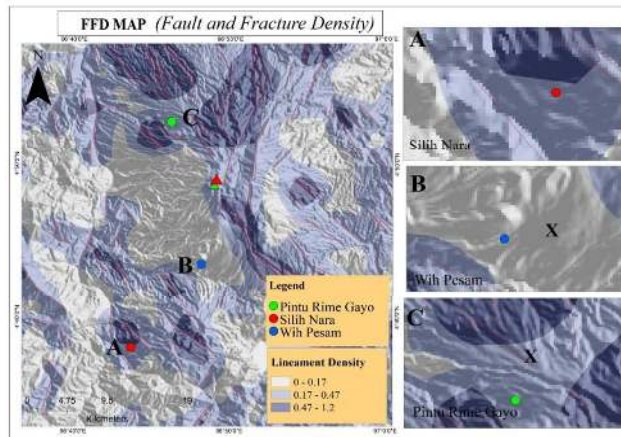


Figure 4. FFD map (Fault and Fracture Density)

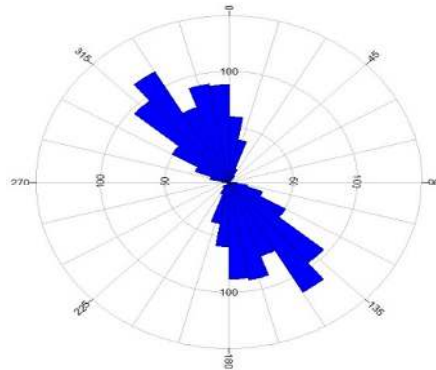


Figure 5. Rose diagram depicting direction and density of faults and fracture

In figure 5, it is known that the dominant straightness direction includes straightness spread along the North-South and Southeast-Northwest of Mount Geureudong. The dominant straightness found in that direction is more than 300 straightness structures, both in faults and cracks. In contrast, straightness with the smallest number has an East-West direction with less straightness than 100.

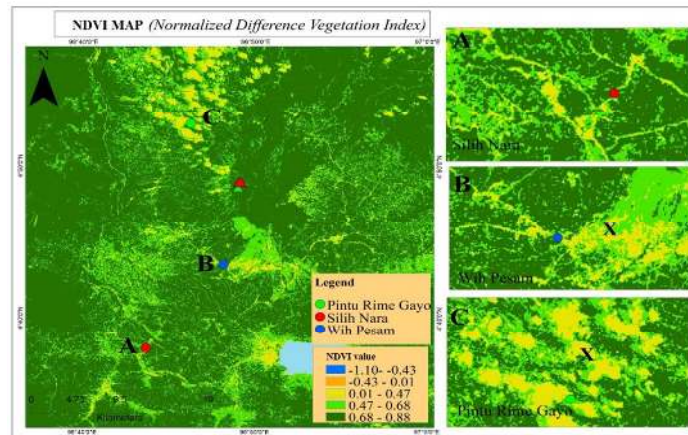


Figure 6. NDVI map (Normalized Differential Vegetation Index)

The results show that the NDVI value in this area ranges from -1.10 to 0.88. It shows that most of the area is covered by vegetation in the form of forests, plantations, and settlements, and there is also a lake in the Southeast (figure 6). The land surface temperature was obtained using the emissivity method of calculating the NDVI (Endah, J. et al., 2017). The NDVI value ranges from -1 to 1. The value of -1 is represented as an area without vegetation. Meanwhile, the value 1 is represented as an area with very dense (good) vegetation. The threshold values for soil (< 0.5854) and vegetation (> 0.5854) were chosen based on the pixel's brightness values from the NDVI image (Hilmi, 2017). The minimum NDVI value with a range of values from -1.10 to -0.43 is indicated in blue on the map. This minimum value is interpreted as a water area or body of water around the research area in the form of a lake. It is clear because the lake area is not

overgrown with plants. Figure 6 also shows the value of vegetation density which is interpreted as sparse vegetation. This value ranges from 0.01 - 0.47, which is symbolized by yellow. The area is interpreted as an area with a low level of plant growth. It is at a sparse to moderate vegetation level for geothermal manifestation points, either in hot springs or fumaroles or the potential distribution of geothermal energy. The geothermal manifestations with sparse vegetation levels (low NDVI) are found in the Pintu Rime Gayo area (North Geureudong), the Wih Pesam area (South of Geureudong) and the Silih Nara area.

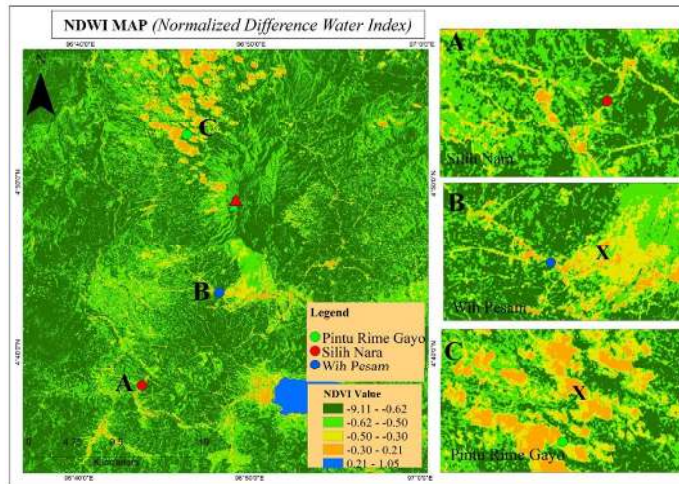


Figure 7. NDWI map of the study area

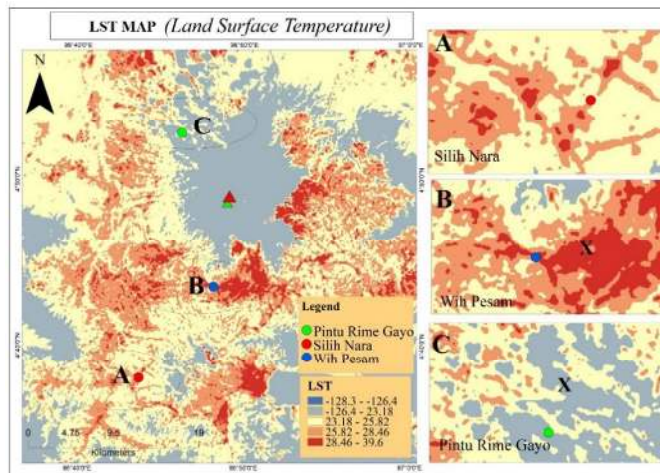


Figure 8. Surface temperature distribution map

In figure 7, it is known that the minimum NDWI value ranges from -9.11 to -0.62, which is symbolized by dark green. This minimum value is interpreted as a tightly vegetated area. Then a value that ranges from -0.62 to -0.50 is interpreted as a moderately vegetated area, which is symbolized by light green. The areas

symbolized in yellow are areas that are rarely vegetated, with values ranging from -0.50 to -0.30. The orange-coloured symbol is interpreted as an open land area or settlement with an NDWI value range between -0.30 to 0.21.

Meanwhile, the maximum NDWI value ranges from 0.21 to 1.05, symbolized by the colour blue. This maximum value is interpreted as water area and water body. The object with this maximum value is a lake located southeast of Mount Geureudong. In the NDWI method, the focus of the calculation is to obtain areas that are identified as waters, either in the form of rivers, lakes, or other watercourses. Based on figure 8, the surface temperature value ranges from -128.3 °C to 39.6 °C. This surface temperature is symbolized by light blue color to dark red. The maximum surface temperature values range of 25.82°C (bright red color symbol) to 39.6°C, which is indicated by the dark red color. The manifestation area and the potential point of geothermal distribution are at this high surface temperature. Although not all include geothermal potential, some locations are man-made objects, such as urban areas that are able to provide high temperatures when viewed via satellite (Cesarian et al., 2018). The manifestation areas with high surface temperatures are Silih Nara and Wih Pesam areas.

For areas with a minimum surface temperature, it has a value of -128.3 °C and is denoted by dark blue. The area has a high level of vegetation density as it is well known that in geothermal, surface temperature has a very close relationship with the level of vegetation density. An area with a high level of vegetation density will have a low surface temperature value and vice versa. If the area has a sparse level of vegetation, the surface temperature value will be higher. This minimum surface temperature value is the cloud point located to the east of Mount Geureudong.

Conclusion

The morphological conditions of the Mount Geureudong area consist of fault structures and dominant fractures that have a West-East and Northwest-Southeast direction. The geothermal potential distribution area is with moderate density (FFD) (0.17-0.47 km / km²), covering the Silih Nara and Pintu Rime Gayo areas. The results of the NDVI calculation show that the research location area has a good land cover with a dominance of moderate to high vegetation density levels. The location of geothermal manifestations is in areas rarely vegetated (Wih Pesam and Pintu Rime Gayo areas) and medium-vegetated areas (Silih Nara Region). The results of the NDWI transformation calculation show that the potential area for geothermal distribution is at a low NDWI value. The maximum surface temperature value in the area of potential geothermal distribution in the Mount Geureudong area ranges from the range of 25.82°C to 39.6°C, which covers the Silih Nara and Wih Pesam areas with the temperature distribution of geothermal potentials being dominated in the Southwest direction of Mount Geureudong. Overall, based on the available data of all the study areas, the highest possibility

to have geothermal potential is Wih Pesam. The area has sparse vegetation based on NDVI and NDWI map and has a high-temperature surface based on the LST map.

Acknowledgement

The research was funded by Grant PNPB 2021 Universitas Syiah Kuala number 172/UN11/SPK/PNPB/2021 Date 22 February 2021. The authors wish to thank for assistance during the data acquisition and thanks to anonymous reviewers for many valuable comments for this paper.

References

- Azhari, P. A., Maryanto, & S. Rachmansyah, A. (2016). Identification of Geological Structure and Its Impact to Land Surface Temperature Based on Landsat 8 Data on Blawan Geothermal Field. *Jurnal Penginderaan Jauh dan Pengolahan Data Citra Digital*, 13(1), 1-12.
- Cesarian, D. P., Abir, I. A., & Isa, M. (2018). Comparison of In-Situ Temperature and Satellite Retrieved Temperature in Determining Geothermal Potential in Jaboi Field, Sabang. In *Journal of Physics: Conference Series* (Vol. 1116, No. 3, p. 032008). IOP Publishing.
- Domra, K., Janvier, Noël, D., Danwe, R., Philippe, N. N., & Abdouramani D. (2015). A Review of Geophysical Methods for Geothermal Exploration. *Renewable and Sustainable Energy Reviews* 44. 87–95. doi: 10.1016/j.rser.2014.12.026.
- Gunawan, H. Caudron, C. Pallister, J. Primulyana, S. Christenson, B. Macausland, W. Hinsberg, V. Lewcki J. Rouwet, D. Kelly, P. Kern, C Werner, C. Johnson, J.B. Utami, (2016). New Insights into Kawah Ijen Volcanic System from The Wet Volcano Workshop Experiment, Geological Society London Special Publications, 437, doi /10.1144/SP437.7.
- Hilmi, M. A. B. M. H. (2017). Integration of remote sensing and geophysical data indetecting geothermal potentials in Ulu Slim, Perak. (Master Thesis), USM.
- Hewson, R. Mshiu, E. Hecker, C. van der Werff, H. van Ruitenbeek, F. Alkema, D. van der Meer, F. (2020). The application of day and night time ASTER satellite imagery for geothermal and mineral mapping in East Africa. *Int J Appl Earth Obs Geoinformation*. 85, <https://doi.org/10.1016/j.jag.2019.101991>
- Isa, M. Dwiky P. Ismail A, Elin Y. Syukri S, Muksin, U. (2020) Remote Sensing Satellite Imagery and In-Situ Data for Identifying Geothermal Potential Sites: Jaboi, Indonesia. *Int. Journal of Renewable Energy Development* 9 (2) 2020: 237-245

- Isaya, N. M., & Avdan, U. (2016). Application of open source coding technologies in the production of land surface temperature (LST) maps from Landsat: a PyQGIS plugin. *Remote sensing*, 8(5), 413.
- Mahmud, M., Muhammad, & Abdullah H. A. (2021). Automatic Mapping of Lineaments Using Shaded Relief Images Derived from Digital Elevation Model (DEM) in Erbil-Kurdistan, northeast Iraq. *Advances in Natural and Applied Sciences*, 6(2): 138-146, 2012 ISSN 1995-0772.
- Nugroho, S. A., Wijaya, A. P., & Sukmono, A. (2016). Analisis Pengaruh Perubahan Vegetasi Terhadap Suhu Permukaan di Wilayah Kabupaten Semarang Menggunakan Metode Penginderaan Jauh. *Jurnal Geodesi Undip*. Semarang.
- Naufal, F., Abdi, S., & Nurhadi, B. (2017). Analisis Estimasi Energi Panas Bumi Menggunakan Citra Landsat 8 (Studi Kasus: Kawasan Gunung Telomoyo) *Jurnal Geodesi Undip*, 6(4). (ISSN: 2337-845X) 371-380
- Endah, J., Sukir, M., & Adi, S. (2017). Pemetaan Suhu Permukaan Tanah Daerah Kawah Wurung, Kabupaten Bondowoso, Jawa Timur Dalam Penentuan manifestasi Panas Bumi. *NATURAL B*, 4(1).
- Nasrullah, Z., Yanis, M., Marwan, & Isa, M. F.V. D. M. (2020). Assessing of Land Surface Temperature at the Seulawah Agam Volcano Area using the Landsat Series Imagery. 0th International Conference on Physics and Its Applications (ICOPIA 2020) *Journal of Physics: Conference Series* **1825** (2021) 012021 IOP Publishing doi:10.1088/1742-6596/1825/1/012021
- Sukendar, P. M., Sasmito, B., & Wijaya, A. P. (2016). Analisis Sebaran Kawasan Potensial Panas Bumi Gunung Salak Dengan Suhu Permukaan, Indeks Vegetasi, dan Geomorfologi. *Jurnal Geodesi Undip Semarang* 5(2), ISSN: 2337-845X.
- Sisay, A. (2016). *Remote Sensing Based Water Surface Extraction and Change Detection In The Central Rift Valley Region of Ethiopia*. School of Natural Resources and Environmental Studies, Wondo Genet College of Forestry and Natural Resources. Ethiopia.
- Ugur, A., & Gordana J. (2016), Algorithm for Automated Mapping of Land Surface Temperature Using LANDSAT 8 Satellite Data. Hindawi Publishing Corporation *Journal of Sensors*, Article ID 1480307, 8 <http://dx.doi.org/10.1155/2016/1480307>.